Ordered Structure in Block Polymer Solutions. 1. Selective Solvents†

Mitsuhiro Shibayama, Takeji Hashimoto,* and Hiromichi Kawai

Department of Polymer Chemistry, Faculty of Engineering, Kyoto University, Kyoto 606, Japan. *Received January 20, 1982*

ABSTRACT: We studied the microdomain structure of a polystyrene–polybutadiene diblock polymer in a selective solvent (*n*-tetradecane, a good solvent for polybutadiene chains (PB) but a poor solvent for polystyrene chains (PS)) as a function of concentration and temperature by using the small-angle X-ray scattering (SAXS) technique with a position-sensitive detector. The microphase separation, giving rise to a microdomain structure composed of spheres of polystyrene chains in a matrix of polybutadiene solution in a regular, simple-cubic-like macrolattice, takes place at a polymer volume concentration $\phi_P > 0.08$ for this particular polymer–solvent system. At low ϕ_P the intersphere distance D_0 varies with $\phi_P^{-1/3}$. The variation of D_0 with temperature T is reversible, D_0 decreasing with increasing T, which is primarily attributed to a decreasing effective repulsive interaction between PS and PB. The temperature dependence of the SAXS profiles indicates that there exist two thermal transitions, at T_d and T_c. The lower temperature transition, T_d, is associated with an onset of line broadening of the SAXS profile as a consequence of a loss of the long-range order in the spatial arrangement of the spherical domains, while preserving the spherical domains. The higher temperature transition, T_c, is associated with extinction of the first-order SAXS maximum as a consequence of an "order-to-disorder" transition, i.e., the microdomain structure being dissolved into a homogeneous mixture. A scaling rule on the temperature dependence of D_0 is derived, $D_0 \sim (1/T)^{1/3}$.

I. Introduction

We have been investigating by small-angle X-ray scattering (SAXS) the microphase separation, the microdomain structure, and the structure of the domain-boundary interphase of polystyrene–polyisophene (SI) diblock polymer materials prepared by solvent casting.[1-8] We now extend our studies to the exploration of the microdomain structure of the block polymers in concentrated solutions for a better understanding of the microdomain structure in the solid state and of the microphase-separation mechanism.

The existence of an ordered structure in block polymer solutions was first reported by Skoulios et al.[9] Further quantitative and systematic studies on the structure of concentrated block polymer solutions have been carried out by Sadron, Gallot, Skoulios, and co-workers[10-14b] and also by Hoffmann and co-workers.[15] Good reviews may be found in papers by Folkes and Keller[14a] and by Gallot.[14b] The microdomain structures in solutions were primarily investigated by SAXS and by electron microscopy coupled with a unique solidifying technique developed by Gallot et al.[10] They used as preferential solvents monomers that could easily be polymerized by irradiation with UV light. The solidified solutions obtained by postpolymerization of the solvent were then cut into ultrathin sections, stained by osmium tetroxide, and investigated by electron microscopy.

However, due to the limited efficiency of the SAXS technique employed in those studies, the studies on the domain structure were conducted only in a relatively narrow concentration range near 100% polymer. Moreover, in most of the cases only the peak positions of the scattering were analyzed to obtain the characteristic spacing. The entire scattering curves were not generally analyzed nor reported in the literature. Owing to recent advances in position-sensitive detectors for X-ray analysis and its related electronics and also of high-flux X-ray sources, one can extend the studies to much lower concentrations (i.e., to systems having much lower scattering power), which can be subjected to quantitative analysis of the microphase separation and resulting microdomain structure.

In this series of works we shall study quantitatively the concentration and temperature dependencies of the microdomain structure developed in a selective solvent (in this paper) and in a nonselective solvent (in a forthcoming paper[16,25]). We shall also discuss (i) the "order-to-disorder" transition, i.e., the thermodynamic transition associated with the dissolution of the microdomain structure by decreasing the concentration below the critical concentration C_c or by increasing the temperature above the critical temperature T_c (in sections III-2 and -3, IV, and V) and (ii) "spatial disordering" of the microdomains at T_d, occurring at temperatures below T_c, which is associated with the loss of long-range order in the spatial arrangement of the spherical domains, while maintaining the domain structure itself (in sections III-3 and V).

This study has been motivated by the work of Watanabe and Kotaka,[17a] who provided insight into the structural origin of the unique rheological behavior of the block polymer solutions to be studied here (i.e., SB in *n*-tetradecane). They suggested from their rheological studies that the nonlinear, plastic flow behavior of the concentrated solutions should be attributed to existence of a superlattice.

The superlattice corresponds to the "ordered structure" in the block polymer solutions studied here, in which spherical domains composed of polystyrene chains are dispersed in a matrix of a polybutadiene solution in a simple-cubic lattice (section III-2, Figures 13 and 14). Watanabe and Kotaka's rheological prediction was unequivocally confirmed and reinforced by our conclusion from small-angle X-ray scattering studies, some results of which have been described in our joint paper.[17b] Although it is our primary objective in this study to pursue a full structural investigation of the block polymer solutions with a selective solvent in order to clarify or predict their physical properties, some conclusions obtained here will further reinforce the prediction drawn from the rheological studies. Some effects of the two structural transitions induced by changing concentration or temperature on the rheological behavior will be described in a forthcoming joint paper.[24]

† Dedicated to Professor Dr. D. J. Meier on occasion of his 60th birthday.

0024-9297/83/2216-0016$01.50/0

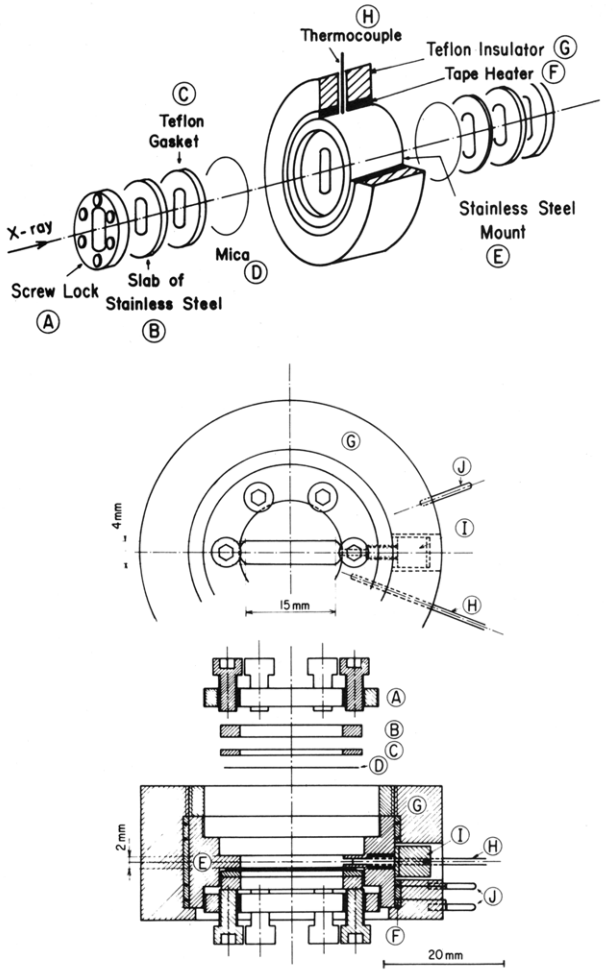

Figure 1. Cell to enclose polymer solutions at various temperatures. Pieces A–H are explained in the figure. Pieces I and J are the inlet for the solution and the terminals of the heater.

II. Experimental Technique

A commercial styrene–butadiene (SB) block polymer (Phillips Petroleum, Solprene 1205) was used as received without further purification. The copolymer has a number-average molecular weight of 5.2×10^4 and styrene content of 29.5 wt %. The solutions studied are *n*-tetradecane solutions (coded as C14), the solvent being highly selective, good for polybutadiene (PB) block chains and poor for polystyrene (PS) block chains. The solubility parameters for PS, PB, and C14 are 9.1, 8.4,[18] and 7.8,[26] respectively. The solutions were prepared by mixing prescribed amounts of the SB copolymer and the solvent with an excess of methylene chloride, which was subseqently evaporated completely to obtain a homogeneous solution of a given concentration. The rheological behavior of these solutions was fully discussed elsewhere[17b] in relation to their microdomain structures.

The solution was enclosed in the cell described in Figure 1. The thickness of the solution along the incident beam is 2 mm. The cell windows are 15 mm high × 4 mm wide and are sealed by thin mica sheets or polyester films D of about 5-μm thickness, which were locked by screw lock A to stainless steel mount E. The solution was heated by tape heater F and temperature was regulated within an accuracy of ±0.5 °C.

The microdomain structure in the solution was investigated as a function of concentration and temperature by small-angle X-ray scattering (SAXS) with a linear position-sensitive proportional counter (PSPC), the detailed description of the apparatus in terms of the optical arrangement of the focal spot, slits, sample, and detector being given elsewhere.[19] The apparatus utilizes a rotating-anode X-ray generator (RU-a, Rigaku-Denki), operated at 55 kV and 200 mA. The SAXS results were corrected for absorption and background scattering (air scattering, parasitic scattering, and the thermal diffuse scattering), nonuniformity of the detector sensitivity, and the collimation errors in both the slit-length and slit-width directions according to a method described elsewhere.[20]

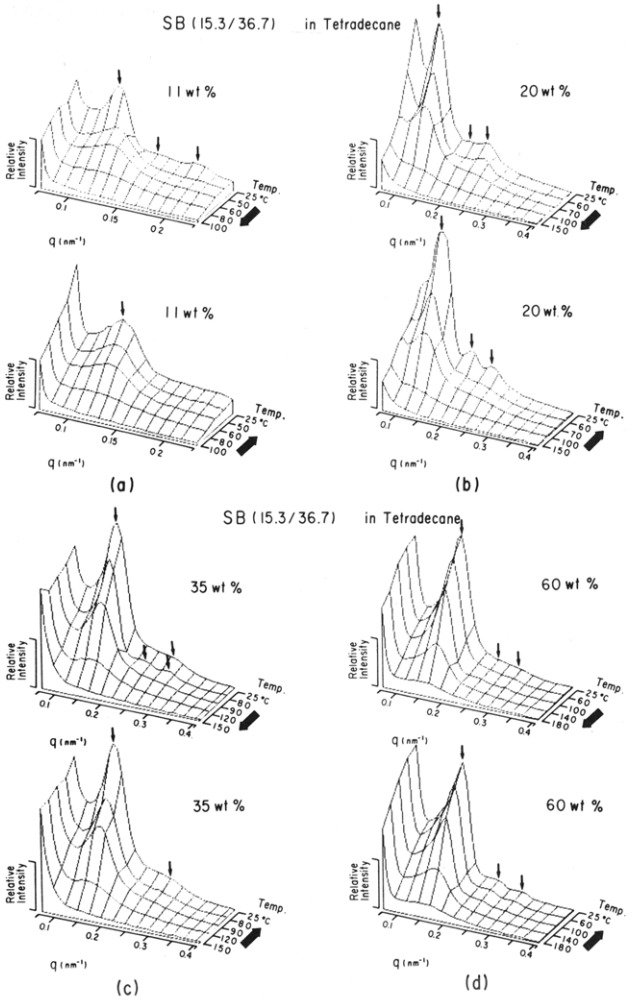

Figure 2. Isometric displays of the uncorrected and smeared scattering curves with temperature and scattering vector q during heating (top row) and cooling processes (bottom row) at 11 (a), 20 (b), 35 (c), and 60 wt % (d) *n*-tetradecane solution of the SB block polymer. The heating and cooling rates are approximately 10 and 5 °C/min, respectively. Each scattering curve was measured with 1000- or 1800-s X-ray exposure time and with 8- or 9-bit position resolution of PSPC.

In order to diminish the effect of history of sample preparation, most of the solution specimens were preheated at a temperature above T_c (where the scattering maximum due to the interdomain distance disappears as will be described in detail later) for about 0.5–1 h. The concentrated solution of 60 wt % polymer was preheated at 150 °C ($T_c > 180$ °C).

III. Experimental Results and Discussion

1. Reversibility of the Structure with Temperature. The reversibility of formation and dissolution of the microdomain structure with temperature was first tested at various concentrations, e.g., 11, 20, 35, and 60 wt % polymer solutions. The results are shown in Figure 2, where are shown isometric displays of the uncorrected and smeared scattering curves with temperature and the scattering vector **q** during heating (top row) and cooling processes (bottom row)

$$|\mathbf{q}| = (4\pi/\lambda) \sin \theta$$

where λ is the wavelength of the X-ray, and 2θ is the scattering angle. The three scattering peaks or shoulders at angular positions of $1:\sqrt{2}:\sqrt{3}$ with respect to the first-order scattering maximum are shown to disappear

Table I
Bragg Spacing D, Radius of the Spherical Domain R As Estimated by SAXS, and Volume Fractions of the Polystyrene Domain

polymer concn, wt %	domain size estimated by SAXS		volume fraction of PS domain				
	D,[a] nm	R,[b] nm	ϕ_{calcd}[c]	ϕ_{sc}[d]	ϕ_{bcc}[e]	ϕ_{fcc}[f]	ϕ_{hc}[g]
8	61.5		0.017				
11	56.7	9.5	0.024	0.020	0.014	0.015	0.058
20	44.7	9.5	0.044	0.040	0.028	0.031	0.094
35	40.1	10.4	0.080	0.073	0.052	0.056	0.140
60	36.2	12.5	0.140	0.172	0.122	0.133	0.250

[a-f] Calculated from eq 1, 2, 8, and 6 (for $k = 1$), 6 (for $k = 2$), and 6 (for $k = 4$), respectively. [g] Calculated for hexagonal close packing of cylinders from eq 9-11.

with increasing temperature and appear reversibly with decreasing temperature. The change of the peak positions is completely reversible, although the change of line profile is irreversible to some extent.

As will be discussed later, the microdomain structure is dissolved into a homogeneous mixture at temperatures higher than the critical temperature T_c, e.g., 95, 105, and 145 °C for 11, 20, and 35 wt % polymer solutions, respectively, and therefore a memory of the solutions should be completely lost at these temperatures.[35] The reversible change of the scattering profiles with temperature as shown in Figure 2 then suggests that the domain structure formed in solution is in an equilibrium state and that its change with temperature also follows closely an equilibrium process.

2. Concentration Dependence. Figure 3 shows the corrected relative scattering intensity distributions with the scattering angle 2θ or s

$$s = q/2\pi = (2 \sin \theta)/\lambda$$

at various polymer concentrations at room temperature. Each scattering curve exhibits a number of scattering maxima or shoulders associated with interparticle interference (the maxima or shoulder marked by thin arrows) and intraparticle interference (those marked by diamond-shaped arrows).

The relative peak positions are $\sqrt{1}:\sqrt{2}:\sqrt{3}:\sqrt{4}$:... with respect to the first-order peak. The peak positions up to the third maximum are generally resolved for all the curves and are marked by arrows. Generally, the third-order peak at $\sqrt{3}$ is more distinct than the second-order peak at $\sqrt{2}$, the latter being smeared in the first-order and third-order peaks, especially for 11 wt % solution. The shoulder associated with fourth-order maximum is discernible for 20, 35, and 60 wt % solutions (the arrows with $\sqrt{4}$). The broad shoulder composed of the sixth- and eighth-order peaks at $\sqrt{6}$ and $\sqrt{8}$, respectively, which overlap each other, is also discernible for 11 and 20 wt % solution.

Existence of the second-order peak located at the position of $\sqrt{2}$ times the peak position of the first-order peak excludes the cylindrical microdomains in the hexagonal close pack, for which the relative peak positions are expected to be $1:\sqrt{3}:\sqrt{4}:\sqrt{7}:\sqrt{9}$:.... The cylindrical hexagonal structure is also excluded from the volume consideration given below. From the volume fraction of polystyrene domain (ϕ_{calcd} in Table I) the polystyrene block chains are considered to be segregated into spheres. Judging from the relative peak positions, the spheres are packed in either a simple-cubic lattice (sc) or a body-centered cubic lattice (bcc). The sc packing seems to be a little bit more probable than bcc because the sc packing yields a closer fitting of the volume fraction of polystyrene domain ϕ_{sc} to that calculated from the concentration and composition ϕ_{calcd} than the bcc packing does (ϕ_{bcc}) (see Table I).

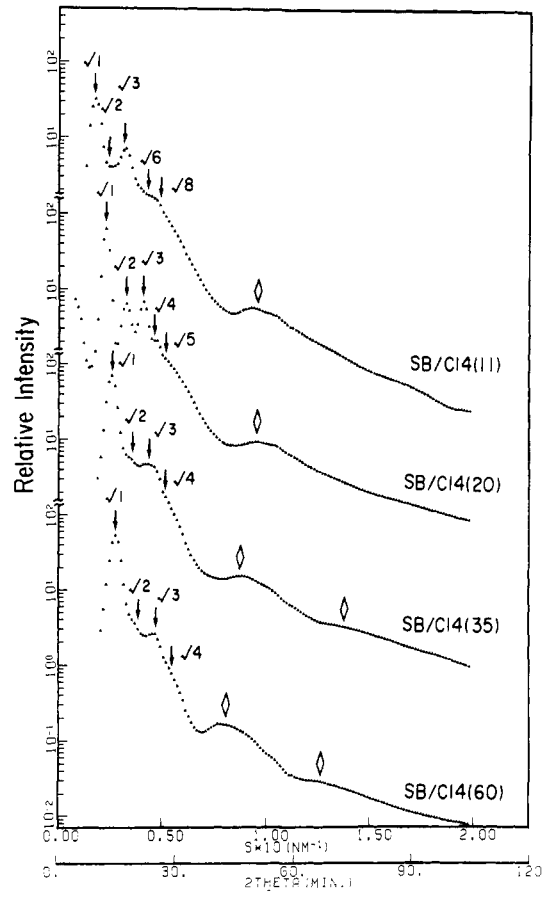

Figure 3. Corrected scattering profiles of the n-tetradecane solutions of the SB block polymer at various concentrations and at room temperature. SB/C14(x) designates x wt % solution of the SB block polymer in n-tetradecane (C14). Each curve was measured with 10 000-s X-ray exposure and 8-bit position resolution of PSPC.

From the scattering angle $2\theta_{max}$ or s_{max} giving rise to the first-order peak, one can estimate the Bragg spacing D

$$2D \sin \theta_{max} = \lambda \quad (1a)$$

or

$$s_{max}D = 1 \quad (1b)$$

One can also estimate the average radius of the sphere R from the nth order scattering maximum $2\theta_{max,n}$ or $s_{max,n}$ from the isolated domain

$$(4\pi R/\lambda) \sin \theta_{max,n} = 2\pi R s_{max,n} = 5.765, 9.10, 12.3, ... \quad (2)$$

for $n = 1, 2, 3, ...$

The values R and D thus estimated are listed in Table I.

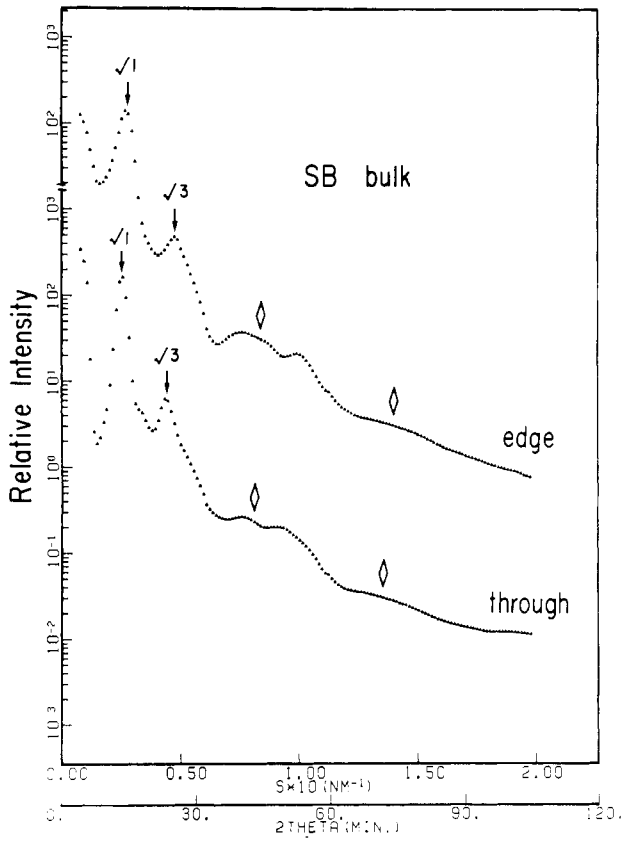

Figure 4. Corrected scattering profiles of the SB block polymer films cast from methylene chloride. The scattering profile was measured by irradiating with the incident beam normal to the film surface (through radiation) and parallel to the film surface (edge radiation). Each curve was measured with 10000-s X-ray exposure and 8-bit position resolution of PSPC.

Now from the Bragg spacing, one can calculate the length of the cell edge "a" of the cubic lattice and also the nearest-neighbor distance D_0 for sc, fcc, and bcc.

$$D = a_{sc} = D_0 \quad \text{(sc)} \tag{3}$$

$$D = a_{fcc}/3^{1/2} = D_0(2/3)^{1/2} \quad \text{(fcc)} \tag{4}$$

$$D = a_{bcc}/2^{1/2} = D_0(2/3)^{1/2} \quad \text{(bcc)} \tag{5}$$

The volume fraction of polystyrene spheres ϕ_k can be also calculated from a and R

$$\phi_k = (4\pi/3)k(R/a)^3 \tag{6}$$

where k = 1, 2, and 4 for sc, bcc, and fcc. The values ϕ_k calculated for sc, bcc, and fcc (defined as ϕ_{sc}, ϕ_{bcc}, and ϕ_{fcc}, respectively) are also listed in Table I.

The volume fraction of polystyrene domain can also be calculated from a given partition fraction of the solvent to polystryrene domain α_{PS} on the basis of no volume change of mixing and of no mixing of unlike segments in each domain,[36] i.e., the polystyrene domains being composed only of the solvent and polystyrene chains and the matrix phase being composed only of the solvent and polybutadiene chains

$$\phi_{calcd} = \phi_P\phi_{PS} + \alpha_{PS}(1 - \phi_P) \tag{7}$$

where ϕ_P is the volume fraction of SB block in the solution and ϕ_{PS} is the volume fraction of PS chains in the block copolymer. In calculating ϕ_{calcd} in Table I, we assumed a complete selectivity of the solvent, i.e., α_{PS} = 0, so that

$$\phi_{calcd} = \phi_P\phi_{PS} \tag{8}$$

and the mass densities of PS, PB, and C14 are 1.052, 0.81, and 0.764 g/cm^3, respectively.

Table II
Estimation of Domain Parameters a and R for Bulk SB Block Polymers Cast from Methylene Chloride

A. Simple-Cubic Lattice

	a_{sc},[a] nm	R,[b] nm	ϕ_{sc}[c]	ϕ_{calcd}[d]
edge	35.1	10.9	0.125	0.26
through	39.9	11.2	0.09	0.26

B. Hexagonal-Close-Packed Cylinders

	a_{hc},[e] nm	R,[f] nm	ϕ_{hc}[g]	ϕ_{calcd}[d]
edge	40.5	9.5	0.20	0.26
through	46.1	9.8	0.16	0.26

[a] Calculated from the Bragg spacing D (eq 1) and eq 3. [b] Radius of sphere calculated from eq 2. [c,d] Volume fraction of sphere calculated from eq 6 and 8, respectively. [e] Cell edge of the two-dimensional hexagonal lattice calculated from eq 1 and 9. [f] Radius of the cylinder calculated from eq 10. [g] Volume fraction of the cylinder calculated from eq 11.

Figure 4 shows corrected SAXS profiles for SB bulk film specimens cast from methylene chloride. The profiles were taken with the incident beam parallel (designated as "edge") and perpendicular (designated as "through") to the film specimens. Comparison of the two profiles indicated that the scattering is nearly isotropic. They have a number of scattering peaks or shoulders attributed to interparticle interference at relative angular positions of 1:$\sqrt{3}$ (they are marked by arrows) and two other peaks attributed to intraparticle interference (marked by diamond-shaped arrows).

The scattering behavior may be interpreted in terms of either spheres in the cubic lattice or cylinders in the two-dimensional hexagonal lattice. However, volume considerations strongly favor hexagonal close packing of the cylinders (Table II). That is, the volume fraction of polystyrene spheres ϕ_{sc} calculated for the simple-cubic lattice is much less than that calculated from the stoichiometry, ϕ_{calcd}.

The cell edge of the hexagonal lattice a_{hc} can be calculated from the Bragg spacing D estimated from eq 1

$$a_{hc} = (4/3)^{1/2}D \tag{9}$$

The radius of the cylinder can also be evaluated from the ith scattering maximum $2\theta_{max,i}$ or $s_{max,i}$ from the randomly oriented isolated cylinders

$$2\pi Rs_{max,i} = 4\pi(R/\lambda)\sin\theta_{max,i} = 5.03, 8.364, 11.585, \ldots \tag{10}$$

$$\text{for } i = 1, 2, 3, \ldots$$

The volume fraction of the polystyrene cylinder ϕ_{hc} can be calculated

$$\phi_{hc} = (2\pi/3^{1/2})(R/a)^2 \tag{11}$$

The volume fraction thus estimated closely agrees with ϕ_{calcd} as shown in Table IIB, suggesting that the bulk SB specimens have a morphology of polystyrene cylinders in a matrix of PB solution in the two-dimensional hexagonal lattice.

The volume fraction ϕ_{hc} in the last column in Table I was calculated by assuming that each polymer solution has a morphology of polystyrene cylinders in a matrix of PB solution in the two-dimensional hexagonal lattice. From the SAXS profiles, a and R were recalculated from eq 9 and 10, respectively, from which ϕ_{hc}'s were also recalculated by using eq 11. The values ϕ_{hc} are much larger than ϕ_{calcd}, indicating that the cubic lattice is much more probable

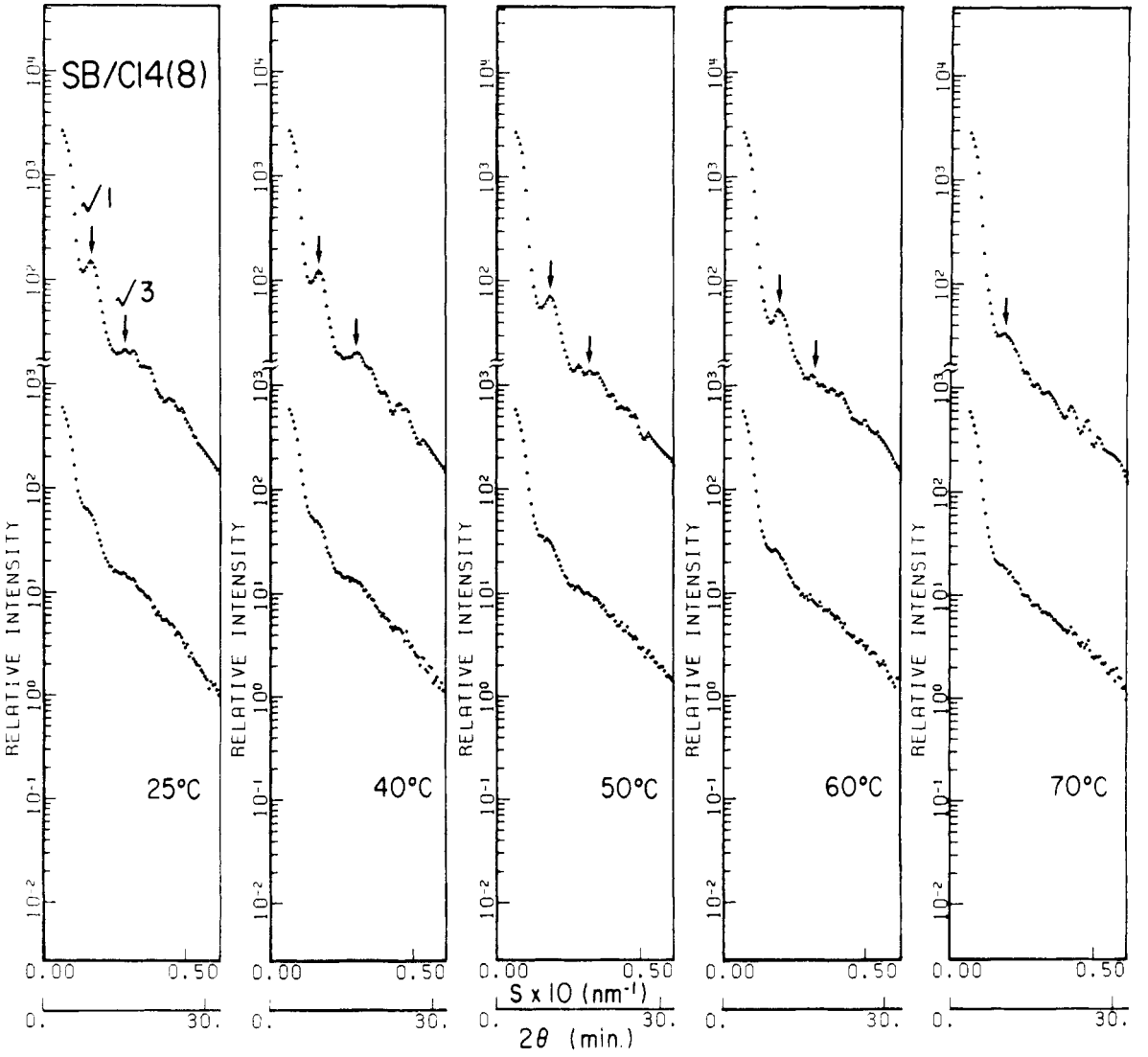

Figure 5. Corrected (top) and uncorrected scattering profiles (bottom) of the 8 wt % solution of the SB block polymer in *n*-tetradecane at various temperatures. Each curve was measured with 500-s X-ray exposure and 9-bit position resolution of PSPC.

Table III
Concentration and Temperature Dependence of the Bragg Spacing for the SB Block Polymers in *n*-Tetradecane Solutions[a]

concn, wt %	temperature, °C													thermal transition, °C	
	25	40	50	60	70	80	90	100	110	120	130	140	180	T_d	T_c
8	61.5	59.0	54.6	52.7	52.7										
11	56.7	56.7	54.2	50.5	49.2	49.2								55	95
20	44.7			43.4	40.1	40.1	39.9	38.8						65	105
35	40.1				37.6	37.6	37.4	36.9	36.2	36.5	35.1			85	145
60	36.2			36.2				36.2				35.8	35.8	125	

[a] The entry at each set of temperature and concentration corresponds to the Bragg spacing in nm.

than the cylindrical hexagonal structure for the solutions. Thus a morphological transition from the PS spheres in the cubic lattice to the PS cylinders in the two-dimensional hexagonal lattice should take place at a polymer concentration greater than 60 wt % for this particular system.

3. Temperature Dependence. In Figures 5–9 are shown the variations of the corrected SAXS profiles with temperature for 8, 11, 20, 35, and 60 wt % C14 solutions of the SB block copolymers, respectively. In Figure 5 are also shown the smeared scattering profiles (the profiles in the bottom at each temperature) as well as the desmeared profiles (the profiles in the top at each temperature).

At low concentration (e.g., 8 wt % solution; Figure 5) only two scattering maxima attributed to the interparticle interference can be detected at relative angular positions of $1:\sqrt{3}$. The first-order peak broadens dramatically in a relatively narrow temperature region centered at T_d (40–50 °C) and disappears at a temperature T_c[28] (about 75 °C in this case), higher than T_d. The two thermal transitions can also be observed at other concentrations; the higher the concentration, the higher the transition temperature (as seen from Figures 5–9 and in Table III). For 60 wt % solution, T_c is higher than 180 °C (see Figure 9).

At higher concentrations (e.g., 11 wt % or greater), the number of the interparticle interference maxima increases. For example, for 11 wt % solution, the four peaks may be discernible at relative angular positions of $1:\sqrt{3}:\sqrt{6}:\sqrt{8}$.

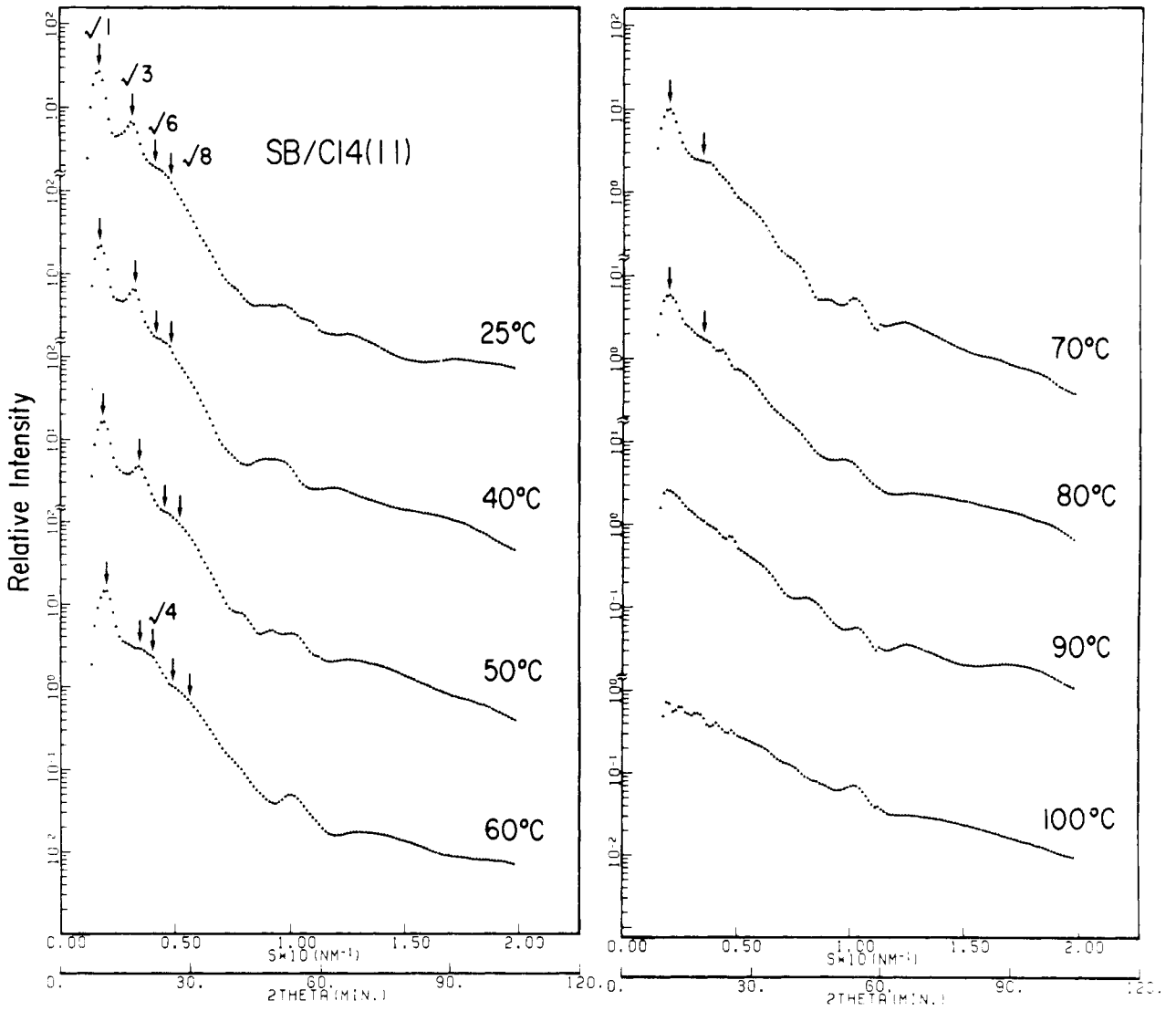

Figure 6. Corrected scattering profiles of the 11 wt % solution of the SB block polymer in *n*-tetradecane at various temperatures. Each curve was measured with 500-s X-ray exposure and 8-bit position resolution of PSPC.

The two peaks at $\sqrt{6}$ and $\sqrt{8}$ overlap into a single broad peak. The peak at $\sqrt{2}$ is smeared between those at $\sqrt{1}$ and $\sqrt{3}$. In order to resolve the peak at $\sqrt{2}$ we need a better resolution as described in detail elsewhere;[20] i.e., the effective length of the PSPC should be resolved into 512 channels rather than 256 channels as employed in this work.[21] The scattering maxima arising from intraparticle interference can only be resolved clearly at 25° C or at the highest about 60 °C (e.g., 20, 35, and 60 wt % solutions). The intraparticle interference maximum drops much faster than the interparticle interference maxima because the intensity decay due to the diffuse boundary between the dispersed domains and surrounding matrix is much greater at larger s than at smaller s and the relative contribution of the thermal diffuse scattering to the net scattering is much greater at larger s than at smaller s.[4-6,8]

The Bragg spacing D was calculated from eq 1 as a function of temperature T at each concentration. The results are plotted in Figure 10 and listed in Table III. The general trend is that the spacing decreases with increasing temperature to a limiting value that is finite but not zero and that seems to depend on concentration (as may be seen from Figures 5–9). The decrease of the spacing with T is primarily attributable to a decreased segregation power, i.e., a decreased Flory–Huggins χ parameter[22] between the PS and PB block chains, causing the PS and PB chains to mix in the PB and PS domains, respectively, and eventually into, more or less, a homogeneous solution. This effect of temperature will be discussed in a more quantitative manner in section V.

IV. Further Analyses on Microdomain Structure as a Function of Concentration

In section III-2 we have shown that (i) the microdomain structure with a long-range spatial order starts to develop at concentrations greater than about 8 wt %, (ii) the microdomain structure formed in the concentration range below 60 wt % SB is spheres composed of polystyrene block chains dispersed in a matrix of polybutadiene solution in a simple-cubic-like lattice, (iii) a morphological transition from spheres in a simple-cubic-like lattice to cylinders of polystyrene block chains in a matrix of polybutadiene solution in a two-dimensional hexagonal lattice should occur at concentrations from 60 to 100 wt % SB, and (iv) the solvent (*n*-tetradecane) has almost a complete selectivity, nearly zero partition of the solvent to PS domains, from the volume consideration ($\phi_{calcd} \simeq \phi_{sc}$ in Table I). The morphological change observed with increasing polymer concentration is a consequence of the increasing volume fraction of the polystyrene phase relative to that of PB plus solvent as discussed by Sadron and Gallot.[10]

Figure 11 shows variations of the Bragg spacing D, which is equal to the cell edge a for the sc lattice, and radius R of the domain with polymer volume fraction ϕ_p. The data

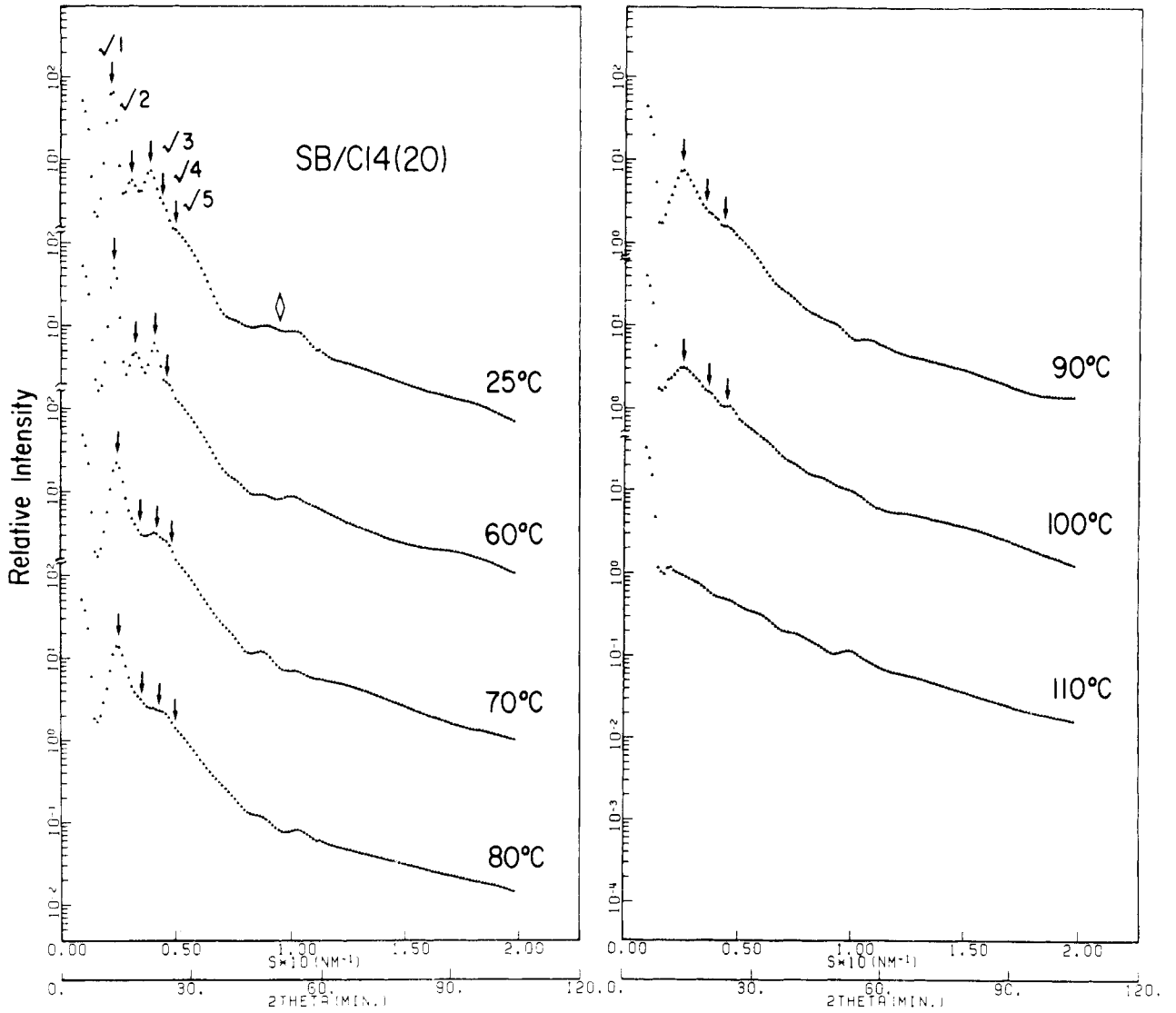

Figure 7. Corrected scattering profiles of the 20 wt % solution of the SB block polymer in *n*-tetradecane at various temperatures. Each curve was measured with 1000-s X-ray exposure and 8-bit position resolution of PSPC.

points marked "t" and "e" at $\phi_P = 1.0$ are those estimated from the SAXS profiles obtained with "through" and "edge" radiation. Naturally, D decreases with increasing ϕ_P. At low concentration D decreases approximately $\phi_P^{-1/3}$ but R does not change significantly; i.e.,

$$D \sim \phi_P^{-1/3} \qquad R \sim \phi_P^{0} \tag{12a}$$

(at low concentrations)

The dash–dot line is calculated from

$$D = D_{20}\phi_P^{-1/3} \tag{12b}$$

where D_{20} is the spacing at 20 wt % polymer concentration.

At higher concentrations, D decreases with ϕ_P at a much slower rate than that given by eq 12a and R increases slowly with ϕ_P

$$D \sim \phi_P^{-0.14\pm0.01} \tag{13}$$

The general trend can be interpreted as a consequence of an increasing number of block chains N per spherical domain, which should result from increased segregation power.[38] That is, with increasing polymer concentration, the system tends to contain fewer bigger spherical domains, leading to a decreased surface-to-volume ratio or average interfacial area occupied by a single chemical junction point of the block polymer S/N, where S and N are the interfacial area and the number of block polymer chains per domain.

On the basis of no volume change of mixing and of pure phases

$$\frac{4\pi}{3}R_{PS}^3 = N\bar{v}_{PS} + \frac{n}{k}\alpha_{PS}\bar{v}_S \tag{14}$$

$$a^3 = kN(\bar{v}_{PS} + \bar{v}_{PB}) + n\bar{v}_S \tag{15}$$

where R_{PS} is the radius of the PS sphere, $\bar{v}_{PS}$, $\bar{v}_{PB}$, and $\bar{v}_S$ are the molecular volumes of PS, PB, and solvent in the solution, respectively, n is the number of solvent molecules per unit cell of volume a^3, and k is the packing constant (1, 2, and 4 for sc, bcc, and fcc, respectively). From eq 14 and 15, one can obtain the relationships[10]

$$\left(\frac{R_{calcd}}{a}\right)^3 = \frac{3}{4\pi k}\,\frac{w_{PS}C/\rho_{PS} + \alpha_{PS}(1-C)/\rho_S}{[w_{PS}/\rho_{PS} + (1-w_{PS})/\rho_{PB}]C + (1-C)/\rho_S} \tag{16}$$

$$\frac{S}{N} = \frac{4\pi k M_t}{CN_A}\,\frac{1}{a}\left(\frac{R}{a}\right)^2\{[w_{PS}/\rho_{PS} + (1-w_{PS})/\rho_{PB}]C + (1-C)/\rho_S\} \tag{17}$$

$$N = \frac{CN_A a^3}{kM_t}\{[w_{PS}/\rho_{PS} + (1 - w_{PS})/\rho_{PB}]C + (1 - C)/\rho_S\}^{-1} \quad (18)$$

where w_{PS} is the weight fraction of styrene in the block polymer, C is the weight fraction of polymer in the solution, ρ_{PS}, ρ_{PB}, and ρ_S are the mass densities of PS, PB, and solvent, respectively, S/N is the average interfacial area per block chain, M_t is the total molecular weight of the block copolymer, and N_A is Avogadro's number.

The values R were calculated from eq 16 by using the measured values of a (=D for a sc lattice) under $\alpha_{PS} = 0$. The calculated values (open triangles in Figure 12) were compared with the values directly estimated from eq 2 (solid triangles). The average interfacial area per chain S/N was also calculated from eq 17 under $\alpha_{PS} = 0$, and the absolute values of N (the number of block chains in a single spherical domain) were estimated directly from eq 14 under $\alpha_{PS} = 0$ by using the measured values of R or from eq 18 by using the measured values of D. These results are summarized in Table IV and Figure 12. Figure 12 contains also the Bragg spacing D (=a for a sc lattice) measured from the SAXS profiles.

It is clearly demonstrated that as the deswelling takes place, i.e., as the concentration C increases, the Bragg spacing D or the cell edge a decreases and N/S (number of block chains per unit interfacial area) or the radius of the PS domain increases, which results from increased segregation power.[38] The close agreement between the calculated R (open triangles) and the observed R (solid triangles) verifies the validity of almost complete selectivity of the solvent; i.e., $\alpha_{PS} = 0$.

Figure 13 illustrates schematically the change of microdomain structure with increasing concentration from $C = 0.11$ (a) to $C = 0.60$ (b). The figure illustrates the structure in the plane cut through the centers of the spherical domains of PS and shows the variations of the cell edge ($D = a$, from 56.7 to 36.2 nm), the radius of the domain (R_{obsd}, from 9.5 to 12.5 nm), and the values of $(S/N)^{1/2}$ (from 2.77 to 2.41 nm). The increase of the value of R or the decrease of the value of $(S/N)^{1/2}$ is a consequence of the increasing number N, due to an increasing degree of segregation.[38] The concentration of PS in the PS spheres is almost 100% irrespective of the overall polymer concentration C, while that of PB in the matrix increases with increasing C.

V. Further Analysis on Microdomain Structure as a Function of Temperature

In section III-3 we found two thermal transitions, i.e., (i) the "lattice disordering" at T_d and (ii) the "dissolution of the microdomain" structure at critical temperature T_c. These two transitions are depicted in Figure 14.[37]

The lattice disordering invokes, more or less, an abrupt broadening of the line profiles of the SAXS peaks as discussed in section III-3 and will be discussed in detail elsewhere.[24] That is, at $T < T_d$, the line width is small and remains almost independent of temperature, thus suggesting that the quasi-elastic potential to maintain the simple-cubic spatial arrangement of the spherical domains is entropic in origin,[24] i.e., the "spring constant" (elastic restoring force per unit displacement) being proportional to k_BT. At $T > T_d$, the line width tends to increase sharply with temperature. That is, at $T > T_d$, the effect of the thermal energy k_BT on the line width outweighs the effect of the spring constant. In other words, k_BT increases much faster than the increase of the spring constant with temperature, resulting in a loss of long-range spatial order. The spherical microdomains themselves and the nearest-neighbor distance D_0 are still well defined below and above T_d. Although the lattice disorder continuously increases with temperature, one may still define the lattice-disordering temperature T_d.

As temperature is further raised to T_c, the segregation power decreases to such a level that the microdomain structure is dissolved into a more or less homogeneous molecular mixture of PS and PB block chains and solvent.[28] This is a kind of order-to-disorder transition. The microdomain structure below T_c confines the chemical junction points of the PS and PB block chains to the restricted spatial volume near the interfaces of the spheres, and, moreover, it confines the orientation of the end-to-end vectors statistically perpendicular to the interfaces, giving rise to an ordered structure. On the other hand, at temperatures above T_c the chemical junction points are distributed randomly in space and the orientation of the end-to-end vectors is also random, giving rise to a disordered structure. Some effects of the thermal transitions of rheological properties were described elsewhere[17b] and will be discussed in a forthcoming paper.[24]

At a given concentration, the domain spacing decreases with increasing temperature, which may be attributed partially to decreasing the statistical segment length with temperature but primarily to decreasing segregation power or the interaction parameter χ_{SB} between PS and PB

$$\chi_{SB} = (\delta_S - \delta_B)^2/\rho_0 k_B T \quad (19)$$

where δ_K is the solubility parameter of K polymer, ρ_0 is the number density of the monomeric unit, and k_B is the Boltzmann constant. If this is the case, the variation of D with T may be essentially and qualitatively described as a function $1/T$

$$D = f(1/T) \quad (20)$$

Figure 15 shows plots of log D vs. log $(1/T)$ at each concentration on the basis of eq 20. Except for the data at the highest concentration (SB/C14(60)), for which the temperature dependence is exceptionally small, the temperature dependence of the solutions at various concentrations has a common feature: (i) the Bragg spacing tends to drop discontinuously at T_d (the T_d's are indicated by arrows in the figure), but (ii) relative temperature dependence below and above T_d is about the same and can be described by

$$\mathrm{d}\log D/\mathrm{d}\log T \simeq -1/3$$

or

$$D \sim (1/T)^{\sim 1/3} \quad (21)$$

for all concentrations.

We propose here that this discontinuity of the Bragg spacing D above and below T_d is just an artifact resulting from the erroneous application of Bragg's law for the disordered structure above T_d as discussed in detail by Guinier[23] and as will be discussed in detail in a forthcoming paper.[24] The spacing D below T_d has a well-defined physical meaning and is identical with the cell edge a or the nearest-neighbor distance D_0 for the simple-cubic lattice. However, above T_d, long-range spatial order is lost and consequently the Bragg law cannot be rigorously applied. Hence the spacing thus estimated does not have a definite physical meaning. Taking this discontinuity into account, one can establish a scaling law of D with T as given by eq 21. This scaling law for the selective solvent turns out to be identical with that for the common solvent,

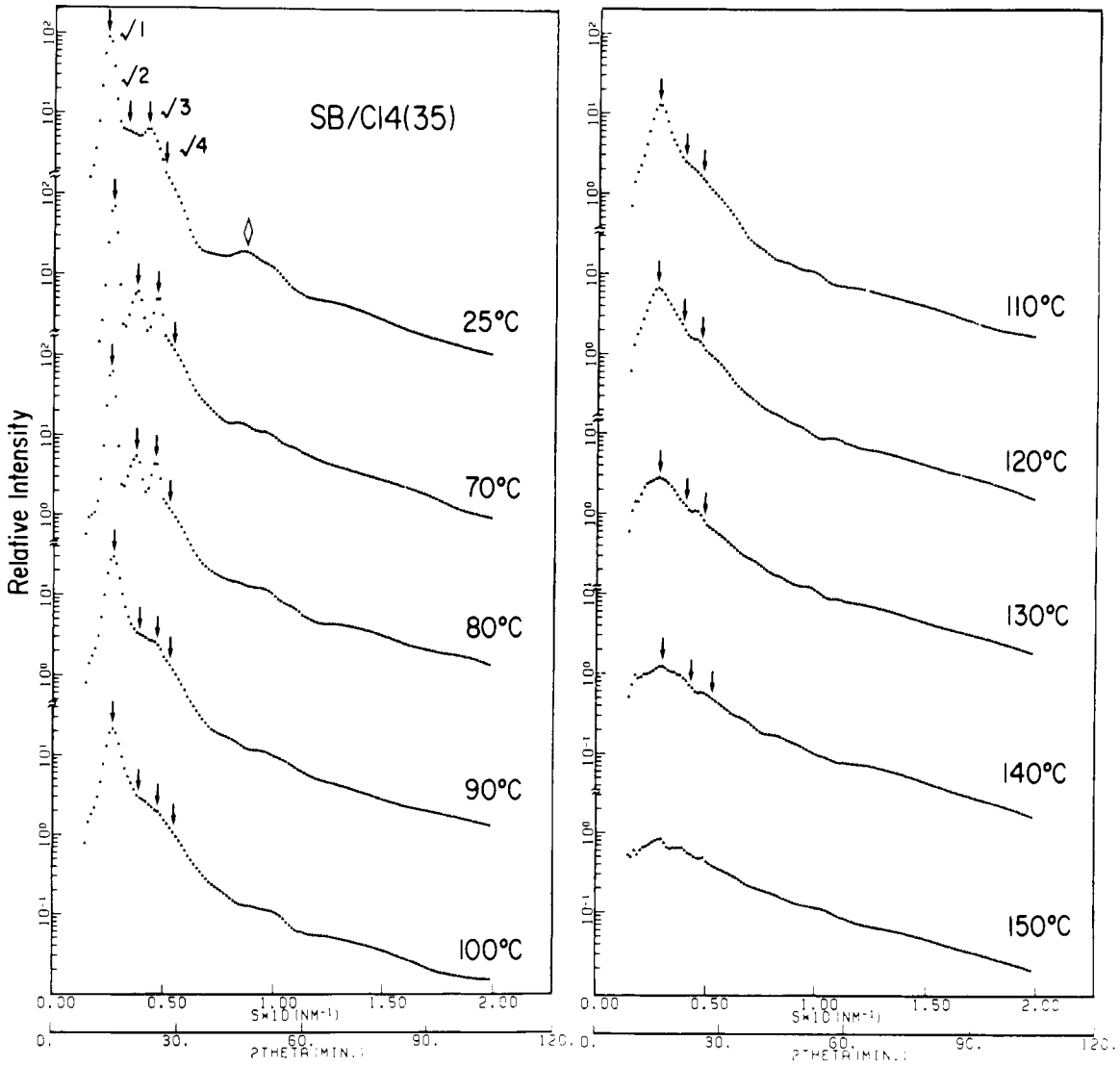

Figure 8. Corrected scattering profiles of the 35 wt % solution of the SB block polymer in *n*-tetradecane at various temperatures. Each curve was measured with the same conditions as in Figure 7.

Table IV
Characteristic Parameters of the Domain as a Function of Concentration

polymer concn		radius of spherical domain, nm		$(S/N)^{1/2}$, nm		N	
wt %	vol %	R_{obsd}[a]	R_{calcd}[b]	calcd[c]	obsd[d]	calcd[e]	obsd[f]
8	6.7		9.9	2.71		167	
11	9.2	9.5	10.2	2.67	2.77	181	148
20	17.0	9.5	9.8	2.72	2.77	164	148
35	30.6	10.4	10.7	2.60	2.64	213	195
60	55.2	12.5	11.8	2.48	2.41	282	338

[a] Calculated from eq 2. [b] Calculated from D (eq 16 under $\alpha_{PS} = 0$). [c] Calculated from D (eq 17). [d] Estimated from R_{obsd} (eq 14 under $\alpha_{PS} = 0$). [e] Calculated from D (eq 18). [f] Estimated from R_{obsd} (eq 14 under $\alpha_{PS} = 0$).

but the scaling law of D with ϕ_p (polymer volume fraction) turns out to be completely different for a different type of solvents[16,25]

$$D \sim (\phi_P/T)^{1/3} \quad \text{(for common solvent)} \quad (22)$$

Thus as far as the temperature dependence is concerned, we may obtain the universal relation of eq 21 irrespective of the solvents, provided that no morphological transition occurs with concentration or for a given morphology. The reason the 60 wt % solution shows a very low temperature dependence is not well understood at present.

Figure 16 shows a schematic diagram summarizing a general feature on the temperature dependence of the microdomain. With increasing temperature, the segregation power between the PS and PB chains decreases so that the A (B) chains can take some walks in the B (A) domains, resulting in decreasing end-to-end distances of the A and B chains, a more spherically symmetric spatial distribution of segments, and increasing average nearest-neighbor distance between the chemical junction points $(S/N)^{1/2}$. Thus the interdomain distance decreases with temperature, which should be accompanied by a decreasing domain radius R, i.e., a decreasing number of block chains N per domain, and also by an increasing thickness of the domain boundary region. This gradual decrease of the segregation power involves the lattice disordering and eventually the order-to-disorder transition of the microdomains.

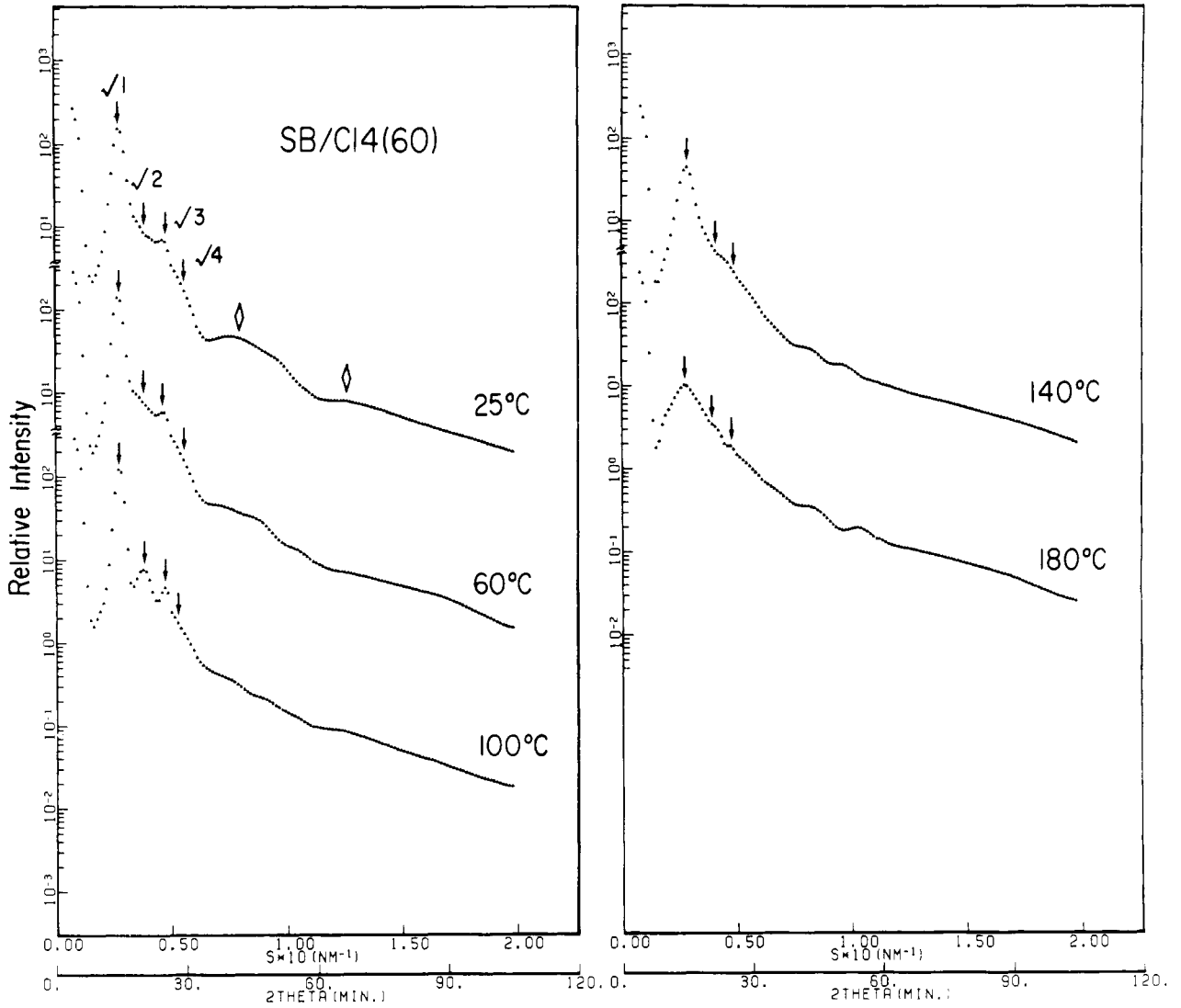

Figure 9. Corrected scattering profiles of the 60 wt % solution of the SB block polymer in *n*-tetradecane at various temperatures. Each curve was measured with the same conditions as in Figure 7.

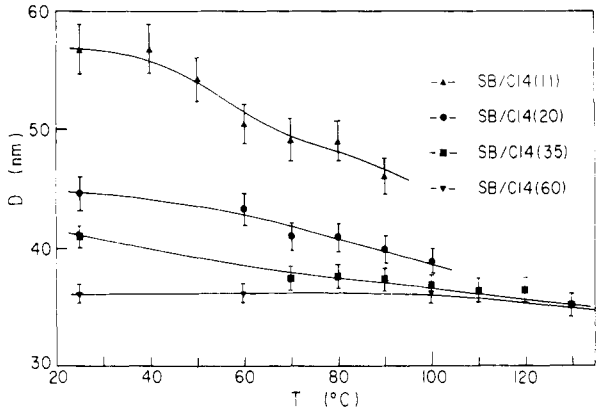

Figure 10. Temperature dependence of the Bragg spacing D for solutions of SB block polymer at various concentrations: (▲) 11 wt % (SB/C14(11)), (●) 20 wt % (SB/C14(20)), (■) 35 wt % (SB/C14(35)), and (▼) 60 wt % (SB/C14(60)).

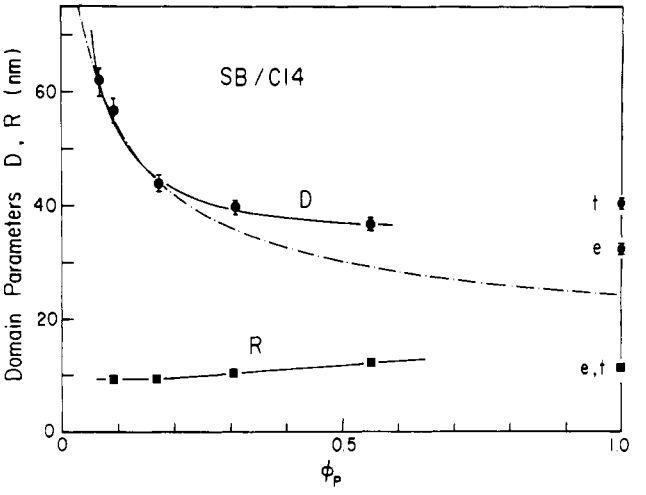

Figure 11. Bragg spacing D and radius R of the spherical microdomains as a function of polymer volume fraction ϕ_p at room temperature. The dash–dot line indicates the change of D with ϕ_p according to eq 12b. The data at $\phi_p = 1.0$ marked by "t" and "e" are the values estimated from the curves obtained by through and edge radiation.

VI. Some Comparisons with Previous Results

Here we will briefly compare our results with those obtained by Sadron and Gallot,[10] Douy and Gallot,[13] Douy, Mayer, Rossi, and Gallot,[12] and Gallot.[14] They systematically investigated microdomain structures in solution in selective solvents as a function of concentration. Especially their studies were focused on morphological transitions among A spheres in B, A cylinders in B, alternating lamellae of A and B, B cylinders in A, and B spheres in A matrix. Their studies focused also on the change of the interdomain distance D_0 and the change of the characteristic parameters derived from D_0 (such as the

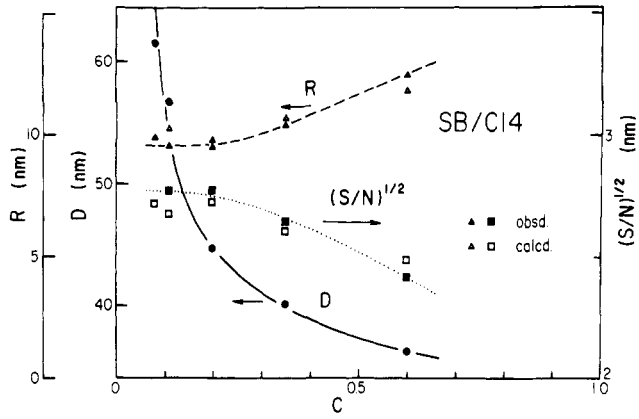

Figure 12. Domain spacing D, domain radius R, and square root of the average interfacial area occupied by a single block chain (S/N) as a function of weight fraction of polymer C. The data marked by solid triangles are estimated from eq 2, while the data marked by open triangles are calculated from eq 16 under the condition $\alpha_{PS} = 0$ (i.e., complete selectivity of the solvent). The data marked by open squares are calculated from the measured a (eq 17), while those marked by solid squares are estimated from the measured R (eq 14).

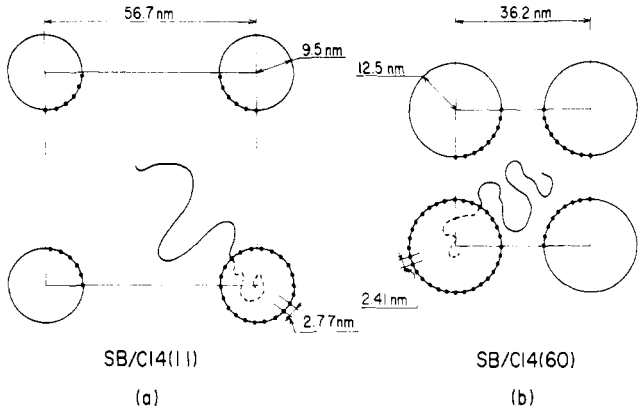

Figure 13. Schematic illustration of the variation of the microdomain structure with increasing concentration from $C = 0.11$ (a) to 0.60 (b). The figure illustrates the structure in the plane cut through the centers of the spherical domains and shows the changes of the cell edge, the radius of the domain, and the average value of $(S/N)^{1/2}$.

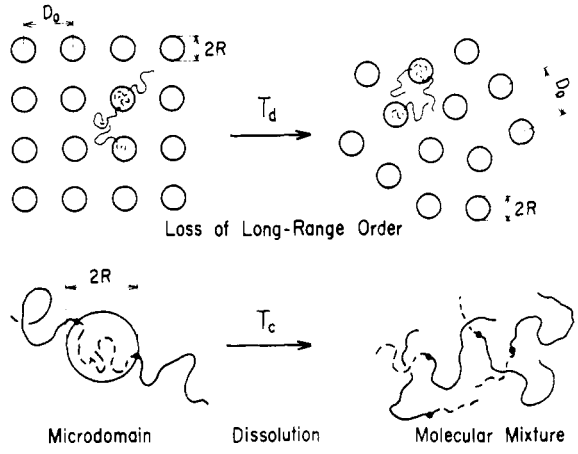

Figure 14. Schematic illustration of the two thermal transitions: (i) the lattice disordering at T_d, which is associated with the loss of the long-range spatial order of the domains (top), and (ii) the order-to-disorder transition at T_c, which is associated with dissolution of the microdomains into a more or less homogeneous molecular mixture (bottom).

radius of the sphere or cylinder R, the thickness of each lamella d_A and d_B, and S/N) with concentration for a given

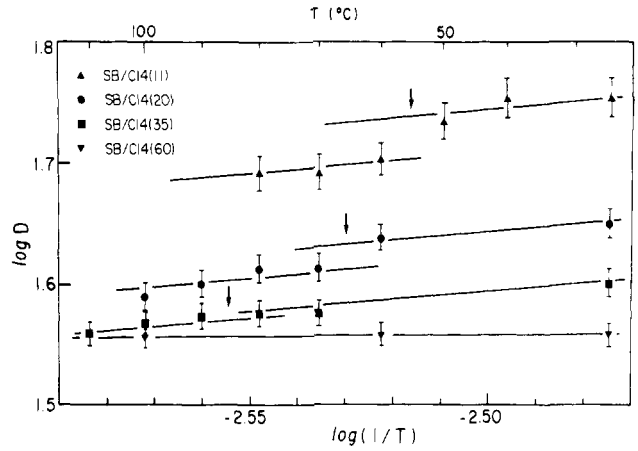

Figure 15. Plot of log D vs. log $(1/T)$ for 11 wt % (SB/C14(11)), 20 wt % (SB/C14(20)), 35 wt % (SB/C14(35)), and 60 wt % (SB/C14(60)) solutions of the SB block polymer in n-tetradecane. The Bragg spacing tends to drop discontinously at the T_d's, i.e., at the lattice disordering temperatures, that are indicated by the arrows in the figure.

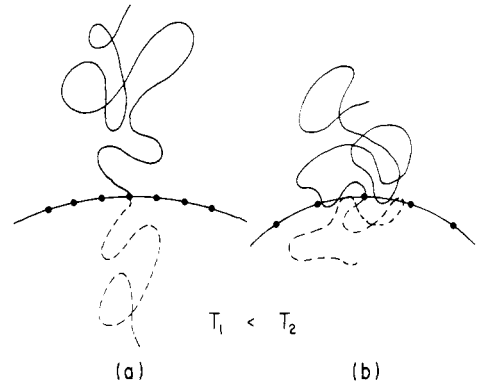

Figure 16. Schematic illustration of the temperature dependence of the microdomain. With increasing temperature from T_1 to T_2, the A (B) chains tend to take some walks in the the B (A) domain, resulting in decreasing end-to-end distances of the block chains, a more spherically symmetric spatial distribution of the segments, and an increasing average nearest-neighbor distance between the chemical junction points $(S/N)^{1/2}$.

morphology. Most of the works in the latter aspects were carried out for the cylindrical or lamellar domain systems, and only a few works focused on the spherical domains.

Obviously, it is not our primary objective in this paper to study the mechanism of the morphological transition with concentration but we are interested in the concentration dependence of the domain parameters D_0 and R for a given morphology (spherical microdomains in this study). Generally, their results on the concentration dependence of D_0 and R for the cylindrical and lamellar morphology can be interpreted in terms of a balance between the lateral and longitudinal dimensional change with concentration. The lateral dimensional change is associated with the change of the parameter S/N while the longitudinal dimensional change is the change of the dimension in a direction normal to the interfaces between the coexisting phases.

Douy et al.[12] reported the concentration dependence of the spherical domains for polystyrene–polyisoprene in solution in isoprene monomer, which is selectively good for polyisoprene where PS domains are dispersed in a matrix of polyisoprene solution in a centered cubic lattice. They indicated that the cell edge a decreases with increasing polymer concentration C. The tendency qualitatively agrees with our results. Although their studies were limited to a narrow concentration range near 100%

polymer ($C \gtrsim 0.7$), we could extend our studies down to very low concentration, $C \gtrsim 0.08$, from which the concentration dependence such as given by eq 12 and 13 was obtained. Douy et al. further estimated R and S/N from the measured values of a (eq 16 and 17) and showed that R increases and S/N decreases with increasing C, which again agree with our results. In our studies we could estimate the radius R directly from the scattering maxima arising from the intraparticle interference (eq 2) and independently from the value a, the information of which is then very useful to determine the selectivity of the solvent i.e., $\alpha_{PS} \simeq 0$. We could draw also the conclusion that the increase of R is a consequence of increasing N, resulting from the system achieving more complete segregation.

Douy and Gallot[13] reported briefly the temperature dependence of the domain parameter D or D_0 and of S/N calculated from D for rod and lamellar systems. They showed that D decreases but S/N increases with increasing temperature, the tendency of which again qualitatively agrees with our results. We proposed that the general trend can be essentially interpreted in terms of a decreasing segregation power with temperature. Moreover, we derived a scaling rule as given by eq 21. We further found existence of the two thermal transitions at T_d and T_c.

Douy and Gallot reported also the thermal transition at T_c, i.e., the transition associated with the disappearance of the mesomorphic structure (corresponding to the dissolution of the domain structure as depicted in Figure 14) from the exothermic peak in their thermograms (see Figure 26–28 of ref 13) for lamellar and cylindrical microdomains. Although the temperature T_c is a function of total molecular weight, composition, and the interaction parameter χ_{AB} of the block polymers as well as the concentration and the interaction parameters between polymer and solvent (χ_{AS} and χ_{BS}), T_c's reported by them seem to be very low compared to those reported in this work and elsewhere.[8,16,25] The quantitative SAXS analyses seem to bear repeating for their systems.

Acknowledgment. We express our sincere thanks to Dr. Meier for his enlightening comments and also to Professor T. Kotaka and Mr. H. Watanabe, Department of Polymer Science, Faculty of Science, Osaka University, Toyonaka, Japan, for stimulating discussions, which motivated the present studies, and also for kindly supplying the SB samples. A part of this work is supported by a grant from the U.S.–Japan Cooperative Research Program of the National Science Foundation and the Japan Society for Promotion of Science.

Registry No. Butadiene–styrene copolymer, 9003-55-8.

References and Notes

(1) Hashimoto, T.; Nagatoshi, K.; Todo, A.; Hasegawa, H.; Kawai, H. *Macromolecules* **1974**, *7*, 364.
(2) Hashimoto, T.; Todo, A.; Itoi, H.; Kawai, H. *Macromolecules* **1977**, *10*, 377.
(3) Todo, A.; Uno, H.; Miyoshi, K.; Hashimoto, T.; Kawai, H. *Polym. Eng. Sci.* **1977**, *17*, 587.
(4) Hashimoto, T.; Shibayama, M.; Kawai, H. *Macromolecules* **1980**, *13*, 1237.
(5) Hashimoto, T.; Fujimura, M.; Kawai, H. *Macromolecules* **1980**, *13*, 1660.
(6) Fujimura, M.; Hashimoto, H.; Kurahashi, K.; Hashimoto, T.; Kawai, H. *Macromolecules* **1981**, *14*, 1196.
(7) Hashimoto, H.; Fujimura, M.; Hashimoto, T.; Kawai, H. *Macromolecules* **1981**, *14*, 844.
(8) Hashimoto, T.; Shibayama, M.; Fujimura, M.; Kawai, H. *Mem. Fac. Eng., Kyoto Univ.* **1981**, *43* (2), 184.
(9) Skoulios, A.; Finaz, G.; Parrod, J. *C. R. Hebd. Seances Acad. Sci.* **1960**, *251*, 739; Skoulios, A.; Finaz, G. *Ibid.* **1961**, *252*, 3467; Finaz, G.; Skoulios, A.; Sadron, C. *Ibid.* **1961**, *253*, 265.
(10) Sadron, C.; Gallot, B. *Makromol. Chem.* **1973**, *164*, 301.
(11) Skoulios, A. E. In "Block and Graft Copolymers"; Burke, J. J., Weiss, V., Eds.; Syracuse University Press: Syracuse, NY, 1973.
(12) Douy, A.; Mayer, R.; Rossi, J.; Gallot, B. *Mol. Cryst. Liq. Cryst.* **1969**, *7*, 103.
(13) Douy, A.; Gallot, B. *Makromol. Chem.* **1972**, *156*, 81.
(14) (a) Folkes, M. J.; Keller, A. In "The Physics of Glassy Polymers"; Haward, R. N., Eds.; Applied Science Publishers: London, 1973. (b) Gallot, B. *Adv. Polym. Sci.* **1978**, *29*, 87.
(15) Hoffmann, M.; Kämpf, G.; Krömer, H.; Pampus, G. *Adv. Chem. Ser.* **1971**, *No. 99*, 351.
(16) Shibayama, M.; Hashimoto, T.; Hasegawa, H.; Kawai, H. Part 3 of this series, submitted to *Macromolecules*.
(17) (a) Watanabe, H.; Kotaka, T. *Rheol. Prepr., Jpn.* **1980**, *28*, 102. (b) Watanabe, H.; Kotaka, T.; Hashimoto, T.; Shibayama, M.; Kawai, H. *J. Rheol.* **1982**, *26* (2), 153.
(18) Brandrup, J.; Immergut, E. H., Eds. "Polymer Handbook"; Wiley: New York, 1975.
(19) Hashimoto, T.; Suehiro, S.; Shibayama, M.; Saijo, K.; Kawai, H. *Polym. J.* **1981**, *13*, 501.
(20) Fujimura, M.; Hashimoto, T.; Kawai, H. *Mem. Fac. Eng., Kyoto Univ.* **1981**, *43* (2), 224.
(21) The peak at $\sqrt{2}$ tends to be resolved at higher concentrations, i.e., at concentrations greater than or equal to 20 wt %, because the angular separation between the two peaks at $\sqrt{1}$ and $\sqrt{3}$ increases with increasing concentration.
(22) See, for example: Flory, P. J. "Principles of Polymer Chemistry"; Cornell University Press: Ithaca, NY, 1971.
(23) Guinier, A.; Fournet, G. "Small-Angle Scattering of X-rays"; Wiley: New York, 1955.
(24) Hashimoto, T.; Shibayama, M.; Kawai, H.; Watanabe, H.; Kotaka, T. Part 2 of this series, submitted to *Macromolecules*.
(25) Hashimoto, T.; Shibayama, M.; Kawai, H. *Polym. Prepr., Am. Chem. Soc., Div. Polym. Chem.* **1982**, *23* (1), 21. Part 4 of this series, submitted to *Macromolecules*.
(26) This value was estimated based on the additivity of molecular attraction constants according to Small.[27]
(27) Small, P. A. *J. Appl. Chem.* **1953**, *3*, 71.
(28) The determination of the temperature T_c at which dissolution of the microdomains takes place is qualitative and somewhat arbitrary here. This is because dissolution takes place gradually over a wide temperature range and consequently the corresponding SAXS peak intensity also decreases continuously over the corresponding temperature range. T_c is defined here as the temperature at which the intensity I_{max} of the first-order scattering maximum drops to such a level that the first-order peak is hardly discernible. Recently, we found that at $T > (T_c)_{ch}$, I_{max}^{-1} linearly decreases with T^{-1} (where T is absolute temperature) and the Bragg spacing approaches a constant value, independent of T, and that at $T < (T_c)_{ch}$, the drop of I_{max}^{-1} with T^{-1} is much slower than that predicted by the linear decrease.[29] We may interpret the scattering maximum at $T > (T_c)_{ch}$ as a peak in the liquid phase arising from the "correlation hole" effect[30] as proposed theoretically by LeGrand and LeGrand[31] and Leibler[32] and experimentally by Roe et al.[33] for *bulk* block polymers. It may be that the scattering maximum from concentrated block polymer solutions arises also from the correlation hole effect. The deviation from linearity of I_{max}^{-1} vs. T^{-1} at $T \leq (T_c)_{ch}$ is then considered to be indicative of the onset of the order-to-disorder transition. The order-to-disorder transition temperature $(T_c)_{ch}$ thus estimated is 100 and 130 °C for 20 and 35 wt % solutions, respectively, the values being slightly lower than those in Table III. Thus the disappearance of the first-order peak is primarily due to decrease of the intensity (to a level which could be hardly detected as a peak) according to the correlation hole concept but not due to the effect of polydispersity of the block polymer as proposed by Leibler and Benoit.[34]
(29) Hashimoto, T.; Kowsaka, K.; Shibayama, M.; Kawai, H., to be submitted.
(30) de Gennes, P.-G. *J. Phys. (Paris)* **1970**, *31*, 235.
(31) LeGrand, A. D.; LeGrand, D. G. *Macromolecules* **1979**, *12*, 450.
(32) Leibler, L. *Macromolecules* **1980**, *13*, 1602.
(33) Roe, R.-J.; Fishkis, M.; Chang, J. C. *Macromolecules* **1981**, *14*, 1091.
(34) Leibler, L.; Benoit, H. *Polymer* **1981**, *22*, 195.
(35) Those T_c values may be compared with that reported by Roe et al.[33] (100 °C) for bulk SB diblock polymer having total number-average molecular weight of 2.7×10^4 and 25 wt % PS. The value T_c is clearly a function of molecular weight and composition for a given combination, e.g., PS and PB. The block polymer used in this study has a much higher molecular weight, thus giving rise to a much higher T_c than that reported by Roe et al. The presence of the solvent, however, signifi-

cantly lowers T_c as shown in Table III and in Figures 5-9.

(36) This assumption is used only when we qualitatively discuss the concentration dependence of ϕ_{calcd} and the spatial packing of the spherical domains but not when we discuss the temperature dependence of the segregation power and its effect on microdomain structure.

(37) The segregation power between the constituent block chains gradually decreases with increasing temperature, which should result in a gradual "disappearance" of the microdomain structure as will be described typically by eq 21. However, the gradual decrease of the segregation power induces the lattice disordering at $T \sim T_d$ and eventually the dissolution of the microdomains at $T \sim T_c$.

(38) **Note Added in Proof.** Alternatively eq 13 may be interpreted in terms of conformational entropy. A simple deswelling process according to eq 12a results in a strong loss of conformational entropy of polybutadiene chains emanating from the polystyrene spheres due to a decreased volume available to these chains. This loss of entropy is avoided by expanding the size of the spherical domain size because it results in the expansion of the interdomain distance and hence in increasing the volume available to the polybutadiene chains.

Thermoreversible Gelation of Atactic Polystyrene Solutions

Hui-Min Tan, Abdelsamie Moet, Anne Hiltner, and Eric Baer*

Department of Macromolecular Science, Case Institute of Technology, Case Western Reserve University, Cleveland, Ohio 44106. *Received October 26, 1981*

ABSTRACT: Atactic polystyrenes (aPS) with either narrow or broad molecular weight distributions have been found to exhibit thermoreversible gelation in a large number of solvents. Samples with molecular weights from 4×10^3 to 2×10^6 were capable of gelation. Clear, one-phase gels were generally formed above the upper critical solution temperature (UCST); below UCST the gel became turbid, i.e., two-phase. No difference was observed between the gelation (T_{GL}) and melt (T_m) temperatures. At relatively low polymer concentrations microsyneresis occurred, implying a volume contraction. A concentration below which no gelation occurred, termed the critical gel concentration (CGC), was a characteristic of each molecular weight. The dependence of CGC on the molecular weight suggests that chain overlap is a necessary condition for gelation. The sol-gel transition temperature could not be correlated with the polymer-solvent interaction parameter. At present, it appears that specific solvent-polymer interactions are necessary for the onset of gelation. The length of the polymer chain and the molecular structure of the solvent affect the ease of gel formation and gel stability.

Introduction

A polymer gel is a three-dimensional network of flexible chains cross-linked by chemical or physical bonds. Accordingly, gels are classified into two types: irreversible and reversible, respectively. In the latter case, any physical process that favors association between certain sites on different chains may lead to gel formation. In a recent review,[1] de Gennes defines three main possibilities as physical gel-forming agents. One possibility is the presence of helical structures with two or more strands entwined to produce the cross-links necessary for network formation. Formation of microcrystallites, which are incapable of excessive growth, represents a second possibility. A third possibility involves the association of like segments of a copolymer dissolved in a solvent that is good for one segment and poor for the other. This latter association may result in nodular, rodlike, or lamellar cross-linking structures. Although assigning one of these types of associations to a particular gel system is still disputed, the fact remains that a mechanism of physical cross-linking is a necessary requirement for thermoreversible gel formation.

More inclusively, these systems are classified by Flory[2] as polymer networks formed through physical aggregation. The aggregates are seen as predominantly disordered but with regions of local order. From the universal characteristics of all types of gels, Flory infers that they must possess a continuous structure of some sort. None of these theories concerned with the nature of the physical aggregations involved in network formation accounts for the previously observed gelation of aPS.[3] This polymer is not known to possess any of the commonly accepted gel-forming characteristics.[1,2] Controversial questions are thus raised regarding possible local order and the origin of associative interchain interactions of the amorphous macromolecule in its solution, gel, or glassy state.

Table I
Molecular Weight Characteristics of Atactic Polystyrene Samples

$\bar{M}_w$	$\bar{M}_w/\bar{M}_n$	lot no.	source
2.0×10^6	<1.2	14B	Pressure Chemical Co.
9.6×10^5	<1.06		Polymer Laboratory Ltd.
6.7×10^5	<1.15	13A	Pressure Chemical Co.
4.1×10^5	<1.06	300-2	Arro Laboratories, Inc.
2.65×10^5	<1.05		Polymer Laboratories, Inc.
2.0×10^5	<1.06	1C	Pressure Chemical Co.
9.7×10^5	<1.06	4A	Pressure Chemical Co.
3.0×10^4	<1.05		Polymer Laboratories, Inc.
2.0×10^4	<1.1		Polymer Laboratories, Inc.
4.0×10^3	<1.1	11B	Pressure Chemical Co.
2.794×10^5	3.08	DF60915	Dow Chemical Co.

This work concerns the characterization of thermoreversible gelation in aPS solutions. Molecular weight and solvent effects have been considered. At present, because there is no unequivocal explanation for the observed phenomena, the subject is presented in the form of a somewhat detailed question in the hope of stimulating future research into the fundamentals of the macromolecular "structure" in the "amorphous" state.

Experimental Section

A. Materials and Procedure. Narrowly dispersed and polydispersed polystyrene with molecular weights in the range $4 \times$

0024-9297/83/2216-0028$01.50/0